Humidity bias and effect on simulated aerosol optical properties during the Ganges Valley Experiment

Yan Feng[1,*], M. Cadeddu[1], V. R. Kotamarthi[1], R. Renju[2] and C. Suresh Raju[2]

[1]Environmental Science Division, Argonne National Laboratory, Argonne, IL 60439, USA
[2]Space Physics Laboratory, Vikram Sarabhai Space Centre, Thiruvananthapuram 695 022, India

The radiosonde humidity profiles available during the Ganges Valley Experiment were compared to those simulated from the regional Weather Research and Forecasting (WRF) model coupled with a chemistry module (WRF-Chem) and the global reanalysis datasets. Large biases were revealed. On a monthly mean basis at Nainital, located in northern India, the WRF-Chem model simulates a large moist bias in the free troposphere (up to +20%) as well as a large dry bias in the boundary layer (up to –30%). While the overall pattern of the biases is similar, the magnitude of the biases varies from time to time and from one location to another. At Thiruvananthapuram, the magnitude of the dry bias is smaller, and in contrast to Nainital, the higher-resolution regional WRF-Chem model generates larger moist biases in the upper troposphere than the global reanalysis data. Furthermore, the humidity biases in the upper troposphere, while significant, have little impact on the model estimation of column aerosol optical depth (AOD). The frequent occurrences of the dry boundary-layer bias simulated by the large-scale models tend to lead to the underestimation of AOD. It is thus important to quantify the humidity vertical profiles for aerosol simulations over South Asia.

Keywords: Aerosol optical depth and extinction, relative humidity, regional climate model.

SOUTH ASIA, the Indian subcontinent in particular, has persistently high aerosol loadings during most of the year and is one of the regional hotspots for aerosol pollution[1–4]. Aerosols over this region originate mainly from industrial activities, residential cooking, agricultural waste and biomass burnings and transportation, and are mixed with dust and sea-spray particles transported from the adjacent desert and oceanic areas respectively. During their residence time in the atmosphere, aerosols can induce a significant radiative impact on the local energy balance by scattering and absorbing the incoming solar radiation[1,5–7], and can cause severe air quality and human health issues[8]. Furthermore, these aerosols may be transported over long distances to affect the climatology and hydrological cycle at larger scales[9], such as accelerating the retreat of the Himalayan glaciers[10,11] and causing a decline in the snow packs[12]. Therefore, it is important to quantify the aerosol loadings, chemical composition, radiative properties and seasonal cycles over the Indian subcontinent and adjacent areas.

On regional to global scales, chemical transport models or aerosol and climate models have been used extensively to simulate the distribution and transport of aerosols over South Asia based on the compiled emission inventories[13–17]. While these model simulations yield insights on the regional-scale characteristics and radiative impact of aerosols, they are often subject to large uncertainties in emissions, aerosol parameterization, cloud representation, and meteorological fields that are used to drive aerosol transport and removal[15,18]. As a result, aerosol concentration and optical depth are often underestimated in the large-scale model simulations over the South Asia region in comparison with ground-based and satellite observations[16,18,19]. Using a recent version of the regional Weather Research and Forecasting (WRF) model coupled with a chemistry module (WRF-Chem) and anthropogenic emissions updated for the year 2010 in India, Feng *et al.*[20] showed that the simulated aerosol optical depth (AOD) is still underestimated compared with the observations. Moreover, they found that about 83% of the low bias in the AOD is attributable to the calculated aerosol extinctions below ~2 km altitude, and on a regional mean basis, if the under predicted extinctions are filled primarily with absorption by aerosols, the model generates significantly different responses in boundary layer heights, atmospheric water vapour and cloud fields compared with the simulation that attributes all the underestimation in extinction to aerosol scattering. One of the possible reasons for underestimation of aerosol scattering could be due to the humidity bias in regional model simulations.

Using the relative humidity (RH) profiles retrieved by ground-based remote sensors, the present study evaluates the vertical characterization of meteorological fields calculated by the regional WRF-Chem model simulations and the National Centers for Environmental Prediction (NCEP) global reanalysis data, and examines the impact

*For correspondence. (e-mail: yfeng@anl.gov)

of simulated humidity on the model predictions of AOD and aerosol extinction profiles. The outcomes of this study will improve our understanding of factors contributing to the discrepancies between the modelled and observed aerosol optical properties at different altitudes, thus pointing to future directions for improvement of aerosol and climate simulations over South Asia. The WRF-Chem model configuration is described in the next section, followed by a description of the observational datasets. The main results include the analysis and evaluation of RH profiles and precipitable water vapour data from models and observations. Also discussed is the effect of the humidity bias on simulated AOD and aerosol extinction.

Model description

This study uses the same version of the WRF-Chem 3.3 model described in Feng *et al.*[20]. It simulates the spatial distribution and temporal evolution of externally mixed aerosols, including sulphate, black carbon (BC), organic carbon (OC), dust (in five size bins with 0.5, 1.4, 2.4, 4.5 and 8 μm effective radius), and sea salt (in four size bins with 0.3, 1.0, 3.2 and 7.5 μm effective radius). It uses emissions of BC, OC and SO_2 over India for the 2010 inventories available at a resolution of $0.1° \times 0.1°$ for a nthropogenic sources and $0.5° \times 0.5°$ for biomass burning[21]. The total emissions of BC and OC are about 1.12 and 3.06 Gg/year over India respectively. SO_2 emissions are 9.36 Gg/year. Additional sulphate emissions from waste and biofuel burning[22] are also included (about 0.21 Gg/year). Dimethyl sulphide, dust and sea-salt emissions are from on-line calculations[23,24]. Calculations of optical properties of aerosols assume internal mixing[25], including the kappa-based hygroscopic growth of aerosol components[26]. The Rapid Radiative Transfer Model for General Circulation Model[27] schemes are used for shortwave and longwave radiation calculations[28]. Other main physical packages used are given in Feng *et al.*[20], including the Thompson cloud microphysics[29] and the Zhang–McFarlane cumulus parameterization[30]. Aerosol simulations are coupled interactively with the prediction of regional meteorological fields at each time step (72 sec).

The model domain is configured from 55°E to 95°E and 0°N to 36°N, with a horizontal grid spacing of ~12 km and 27 vertical layers. The initial and boundary conditions of meteorological fields are interpolated to the model time step from the 6-h NCEP reanalysis data available at $1° \times 1°$ resolution. Outputs from the MOZART-4 global chemical transport model[31] are used for deriving initial and boundary chemical conditions.

Eight months of WRF-Chem simulations were performed from August 2011 to March 2012, at the same time as when multi-instrumental meteorology and aerosol data were collected by the US Department of Energy (DOE) Ganges Valley Aerosol Experiment (GVAX) at a mountaintop site, Nainital (29°N, 79°E, 1939 m amsl), northern India. The AOD and aerosol extinction profiles generated with the WRF-Chem model have been evaluated by comparison with aerosol observations, as reported in Feng *et al.*[20].

Datasets

In this study, *in situ* and ground-based remote sensing data of RH profiles, temperature, and precipitable water available during GVAX are compared with the WRF-Chem simulations as well as the NCEP reanalysis data. At Nainital, the temperature and RH profiles are derived from radiosondes launched every 6 h (00 Z, 06 Z, 12 Z and 17 Z), and these profiles extend from the surface up to 10 km. Monthly mean profiles are then calculated from the six-hourly data. In addition, RH profiles retrieved from Microwave Radiometer Profiler (MRP) are obtained at Thiruvananthapuram (TVM: 8.55°N, 76.9°E, 75 m amsl and ~200 m inland from the Arabian Sea coast), located in southern peninsular India, from December 2011 to March 2012. Details of the study region, radiometer installation and its mode of operation over TVM are reported by Raju *et al.*[32]. This dataset is available at hourly intervals up to 10 km. Together they provide the high-frequency temporal variations in the temperature and humidity profiles from post-monsoon to winter and pre-monsoon seasons at these two ground sites.

Aerosol extinction profiles and AODs for March 2012 were retrieved at Nainital from the DOE atmospheric radiation measurement mobile facility 1 (AMF1) micropulse lidar (MPL) backscatter measurements at 532 nm wavelength and multi-filter rotating shadow band radiometer (MFRSR) measurements at 500 nm wavelength. The extinction retrievals at 30-min frequency are averaged hourly and monthly with a vertical resolution of ~500 m. They are used for evaluation of the modelled aerosol optical properties together with the post-processed, quality-assured AMF1 AOD products (pghmfrsraod1michM1.s1 datastream) from the MFRSR. The aerosol observations are used together with the relative humidity data to evaluate the humidity effect on aerosol optical properties simulated by the WRF-Chem model.

Humidity bias at Nainital and Thiruvananthapuram

Using the WRF-Chem simulations, Feng *et al.*[20] recently showed that the column AOD and aerosol extinctions at Nainital are underestimated compared with the satellite and ground-based measurements during the pre-monsoon month of March 2012. They speculated that the humidity bias in the regional climate model is one of the factors contributing to this underestimation of aerosol optical

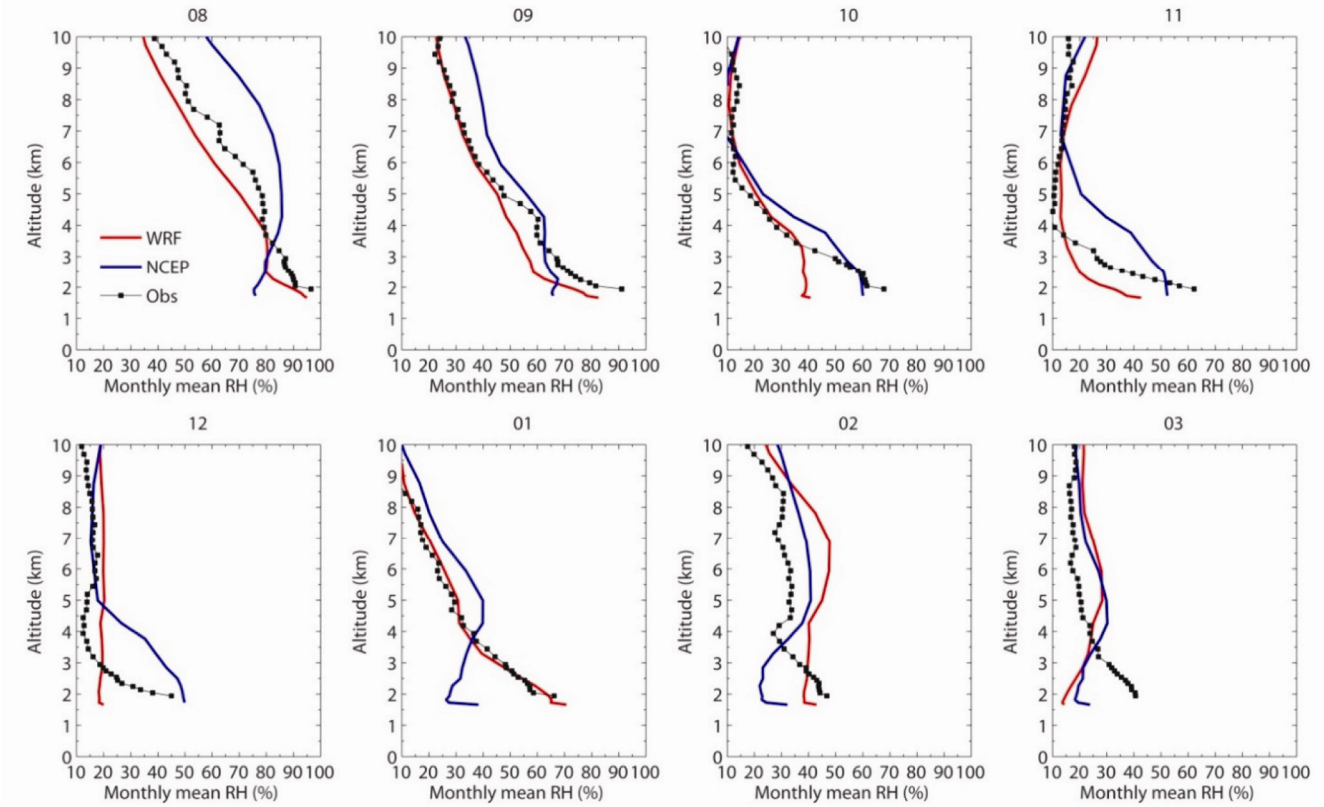

Figure 1. Monthly mean relative humidity profiles at Nainital from the six-hourly radiosondes (Obs), six-hourly NCEP reanalysis data (NCEP), and the hourly WRF-Chem model simulations (WRF) during GVAX from August 2011 (upper left panel) to March 2012 (bottom right panel).

properties. To evaluate the model-simulated humidity profiles, Figure 1 compares the monthly mean RH profiles at Nainital from the 12-km WRF-Chem model and 1° × 1° NCEP reanalysis (interpolated to the 12-km grid cells) with the radiosonde sounding data collected from August 2011 to March 2012. The NCEP reanalysis data are included because they were used to prescribe the initial and boundary meteorology conditions for the regional WRF-Chem model simulations.

From August to November, the wetter monsoon season transitions into the drier post-monsoon. Correspondingly, the atmospheric RH decreases throughout the column from the surface to the upper troposphere. In particular, RH in the free troposphere is low as 10–20% in October and November, compared to about 40–60% on average in August and September. The boundary-layer RH also decreases by 20%, from above 80% to below 60%. These seasonal variations in RH profiles are consistently captured in both the NCEP data and WRF-Chem model. However, the NCEP data overestimate the absolute values of RH in the upper troposphere and underestimate them near the earth's surface compared with the sounding data. The finer grid spacing of the WRF-Chem model better resolves processes in space. This capability leads to better agreement with the observed RH at higher altitudes above the boundary layer, which is about 4–5 km above sea level over this time period. On the other hand, the WRF-Chem model under-predicts RH near the surface, and even produces larger low biases in October and November.

During the winter and early spring months from December to March, the atmospheric conditions at Nainital remain generally dry, with RH values less than 50% near the surface and less than 30% in the free troposphere. In this time-span, January is the only exception, when the monthly mean RH at the surface reaches up to 70% according to the sounding data. This high-RH month is well-simulated by the WRF-Chem model. The occurrences of high RH in January might be related to the frequent formation of upslope winter fog at this site. Interestingly, the high RH does not appear in the NCEP reanalysis data, which suggests much lower mean RH (below 40%) near the surface, possibly because the coarse spatial resolution of the data does not resolve the topography-driven fog formation.

Overall, the WRF-Chem model reproduces the seasonal changes in RH present in the radiosonde sounding profiles over the eight-month period of GVAX, although the regional model results are systematically lower than the observations near the surface by up to –30% on monthly average. This low bias is, in part, inherited from the NCEP data, which are used as initial and boundary meteorology of the regional model. Compared with the NCEP data, the 12-km resolution WRF-Chem model reduces the

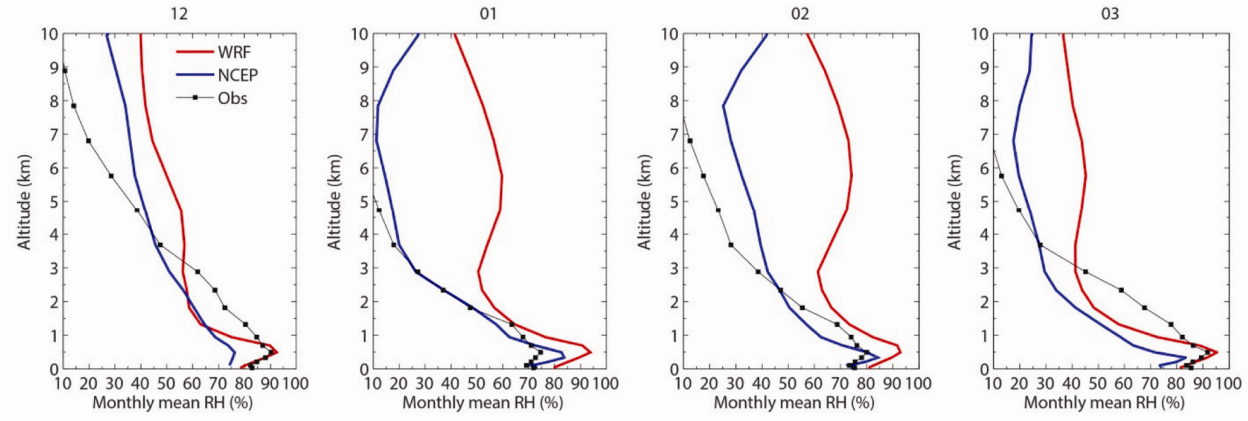

Figure 2. Monthly mean relative humidity profiles at TVM from MRP (Obs), NCEP reanalysis (NCEP), and WRF-Chem model simulations (WRF) from December 2011 to March 2012.

biases in RH for most months, and the improvement is more significant in the upper troposphere than in the boundary layer.

Figure 2 shows the RH profiles for the TVM site. The observed RH profiles at this site exhibit a distinct inversion between the surface and 500 m, which is also depicted by both the WRF model and NCEP data. Compared with Nainital site, the seasonal variations in RH at Thiruvananthapuram are relatively weaker, and the RH values are constantly high (above 70%) in the lower troposphere and decrease as a function of altitude. Due to its proximity to the sea coast and being a coastal station, the vertical distribution of specific humidity at TVM also shows less variability at 0–2 km altitude level[33]. The overall pattern of RH biases in the WRF-Chem model (moist bias in the free troposphere and dry bias in the lower troposphere) is consistent between the two sites, but the magnitude of these biases varies from one location to another. The dry biases in the lower troposphere are generally smaller at TVM than Nainital, especially in the region from the ground to 500 m. In January and February, the WRF-Chem model simulations display boundary-layer wet biases. In the upper troposphere, the magnitude of the wet biases is larger in the WRF-Chem model than in the NCEP data at TVM, in contrast to Nainital.

In spite of these large biases in simulated RH profiles, differences in the column total precipitable water vapour (PWV) are relatively small due to compensation of the upper-layer wet biases and lower-layer dry biases. Figure 3 shows the estimated PWV from the WRF-Chem model versus the sounding data at Nainital from November 2011 to March 2012. The time-averaged difference in PWV is only about 1 mm, and while the WRF-Chem model overestimates the averaged total PWV (6 mm) by ~17%, it is able to reproduce the diurnal variation in water vapour. This conclusion is confirmed by the good agreement in the daytime mean PWV between the microwave radiometer measurements (5.1 mm) and WRF-Chem results (5.9 mm).

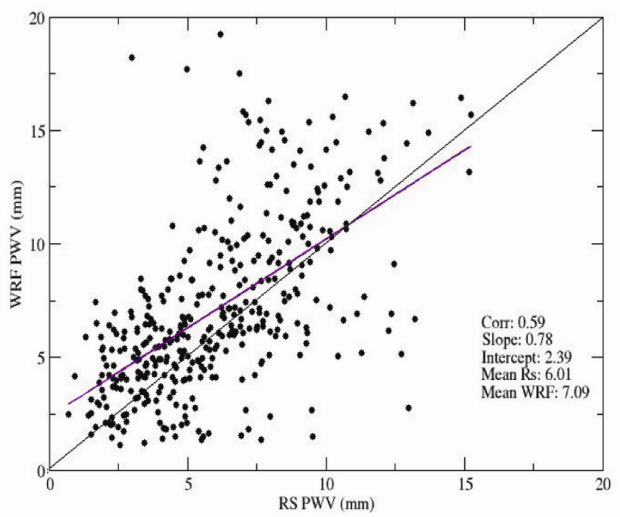

Figure 3. Scatter plot of precipitable water vapour (PWV) from the WRF model vs radiosondes (RS) at Nainital, from November 2011 to March 2012. The purple line is the linear fit of all the data points (slope and intercept are shown in the legend).

Effect of humidity bias on aerosol extinction and AOD

The magnitude of the aerosol extinction coefficients depends strongly on the RH values in the atmosphere[34]. With higher ambient RH, the aerosol particles may grow larger and scatter the incoming solar radiation more efficiently. In WRF-Chem, the kappa-based hygroscopicity method[26] is used to calculate the particle humidity growth for internally mixed multi-component aerosols containing varying amounts of inorganic, organic and surface active compounds. Although the phase state of aerosols in the atmosphere is not precisely known, it seems reasonable to assume that metastable states dominate in the hygroscopic growth of particles, especially because internal mixtures are considered[26]. Then optical properties of aerosol mixtures are calculated based on a parameterization following the Mie theory[25].

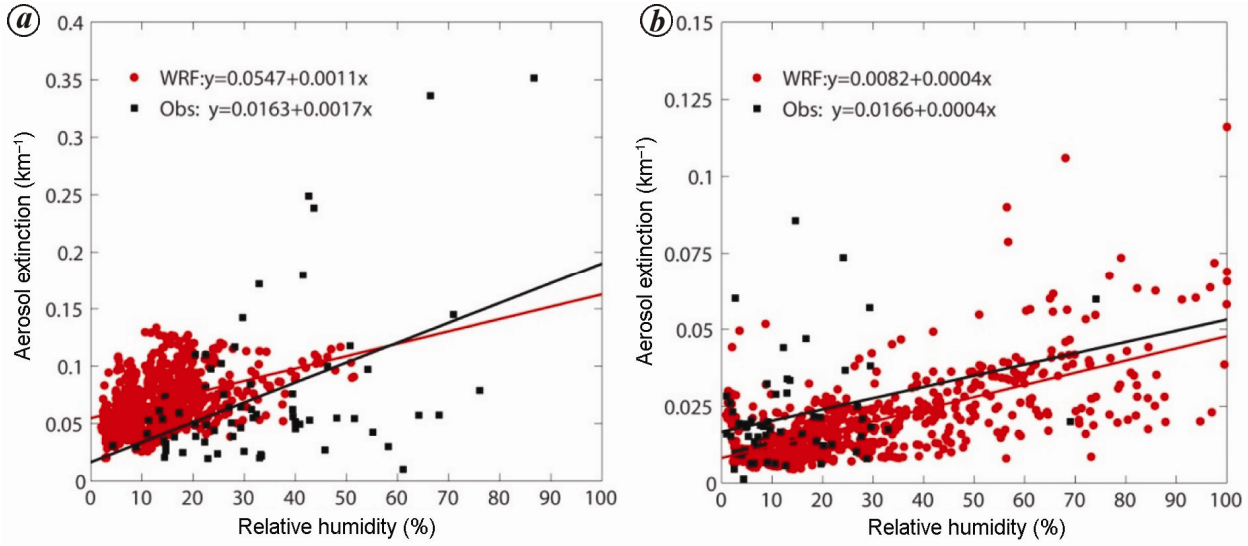

Figure 4. Aerosol extinction as a function of relative humidity at (***a***) the surface and (***b***) 5 km at Nainital for March 2012. Hourly WRF-Chem calculations are shown together with the six-hourly radiosonde humidity data coincident with the available MPL-retrieved extinction coefficients.

Figure 4 shows the observed and simulated relationship between RH and aerosol extinction at Nainital for two levels: the boundary layer (surface) and free troposphere (5 km). The black points represent six-hourly sounding RH data coincident with the available hourly MPL data, and the red points are WRF-Chem outputs (hourly) for March 2012. The red and black lines are best fits of the model results and data. The slope of the linear fit of the data points indicates the average effect of humidity on aerosol extinction. At the surface, the simulated humidity effect on aerosols (slope = 0.0011) is slightly weaker than that inferred from the observed aerosol extinction and RH (slope = 0.0017). The goodness of fit is 0.16 for the model outputs and 0.38 for the observational data. A possible reason for the scatter in the linear fit is that the RH dependence of the aerosol extinction is widespread at the surface due to the diverse chemical composition, size distribution and mixing state of aerosols influenced by a variety of surface emission sources. Even under the same RH conditions, the observations show a large variability in aerosol extinction, which is underrepresented by the WRF-Chem model. Although the empirical relationships based on linear fitting may not fully capture the complexity between extinction and RH, it nevertheless provides a first-order evaluation of the simulated humidity effect on aerosol extinction compared with observations. Note that in the WRF model, this humidity dependence is calculated based on predicted aerosol properties. Compared with the surface level, the effect of humidity on aerosol extinction is considerably weaker at 5 km in both the model and observations (slope = 0.0004), with a better goodness of fit for 0.45 and 0.87 respectively. This finding implies that aerosols in the free troposphere, most likely aged, tend to be more uniform in composition and size, and less hydrophilic than the surface aerosols as those hydrophilic and/or larger particles may have been scavenged by dry and/or wet removal processes during the aging. The data in Figure 4 demonstrate that the WRF-Chem simulations largely reproduce the observed humidity effect on aerosol extinction at different altitudes in the column, despite the dry bias in RH at the surface and wet bias at 5 km. Because the model captures similar slopes of extinction over RH to the observations, it allows us to further examine and quantify the effect of the RH biases on simulated aerosol optical properties.

Earlier Feng *et al.*[20] proposed that the humidity biases contribute to the underestimation of aerosol extinction as a function of altitude and AOD in the WRF-Chem regional simulations. As shown in Figure 5, the vertical profile of monthly mean extinction at Nainital is under predicted for March 2012 by the default WRF-Chem model (control run) compared with both the ground-based MPL and MFRSR retrievals and satellite CALIPSO extinction profiles. In particular, AOD underestimation in the boundary layer (below ~2 km) is more than a factor of two. Since the humidity effect on extinction is similar in the model and data (Figure 4), the predicted aerosol extinction profiles ($b_{\text{ext,control}}(z)$) can be thus scaled by the ratio of the observed RH ($\text{RH}_{\text{obs}}(z)$) over the WRF-modelled RH ($\text{RH}_{\text{control}}(z)$) as a function of altitude (Figure 1) as

$$b_{\text{ext,adjusted}}(z) = b_{\text{ext,control}(z)}(z) \times \frac{\text{RH}_{\text{obs}}(z)}{\text{RH}_{\text{control}}(z)},$$

where z is the model level.

The extinction profile determined by the model (adjusted) is shown by a green line with open circles in

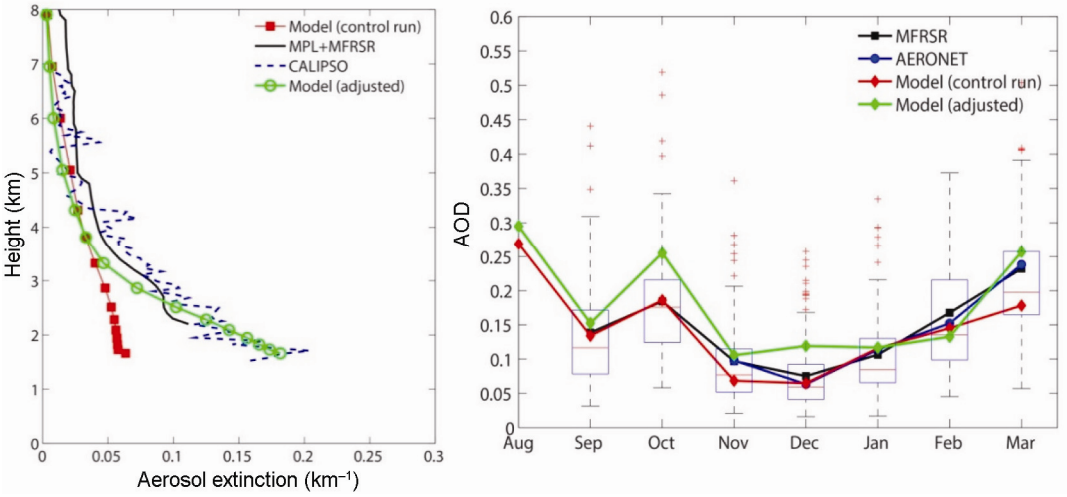

Figure 5. Aerosol extinction and aerosol optical depth (AOD) at the Nainital site. (Left) Monthly mean aerosol extinction profiles for March 2012 from the model control run at 550 nm (red), model adjusted by RH bias (green), ground-based MPL data (black), and satellite-retrieved CALIPSO data (blue). (Right) Monthly mean column AODs from model control run (red), model adjusted by RH bias (green), ground-based MFRSR (black), and AERONET retrievals (blue). Box-whiskers denote the distribution of hourly MFRSR data in each month: red bar for the median; box and whiskers for 1-sigma and 2-sigma values respectively.

Figure 5 (left panel). It agrees with the observed profiles, i.e. within 1% of the CALIPSO data estimated as

$$\frac{\sum_{i=1}^{n} \frac{[b_{\text{ext,model}}(i) - b_{\text{ext,CALIPSO}}(i)]}{b_{\text{ext,CALIPSO}}(i)}}{n} \times 100.$$

This agreement suggests that the low bias in RH is the dominating factor that causes discrepancies between the aerosol extinction predictions from the observations for the case of March 2012 at Nainital.

Similar to the month of March, the bias corrections in RH can be calculated as a function of height based on the sounding data and can then be used to adjust the predicted aerosol extinctions for the other seven months. In the right panel of Figure 5, the calculated monthly mean AODs from the default WRF-Chem model output (control run) and the bias-corrected model output (adjusted) are compared with the ground-based measurements from the MFRSR and AERONET from August 2011 to March 2012. The AOD monthly means are also summarized in Table 1. Consistent with the extinction profile comparison for March, shown in the left panel of Figure 5, application of RH bias adjustment increases the monthly mean AOD from 0.18 (from the control run) to 0.26, which is in better agreement with the AERONET data (0.24) and MFRSR measurements (0.23). A similar improvement in AOD is also found for November due to the correction of low bias in RH. For January and August, since the simulated RH profiles are similar to the observations, the resulting changes in AOD are small. For the remaining three months, especially in October and December, the improvement in RH profiles does not result in a corresponding improvement in AOD, causing instead larger differences between the modelled and observed AODs. This finding indicates that there may be other uncertainties in the predicted aerosol properties (concentration, hygroscopicity, etc.), which were fortuitously offset by the humidity biases in the estimation of AOD. Due to lack of MPL data for other months, we could not examine the simulated aerosol hygroscopic growth as shown in Figure 4 for March. Additionally, errors in simulated boundary-layer dynamics could also have significant impacts. Nair *et al.*[16] suggest that the nonlocal boundary-layer scheme used in their regional climate model (RegCM4) tends to overestimate vertical mixing and thus underestimate the near-surface BC under convectively stable conditions such as night-time and winter. Using a version of the WRF-Chem similar to the present study implemented with a local boundary-layer scheme (Mellor–Yamada–Janjic scheme), Govardhan *et al.*[35] have shown that the model also overestimates the surface wind speed and boundary-layer height compared with the MERRA reanalysis data, and such overestimations correlate with the surface BC under predictions. Our study provides another possible explanation by demonstrating that correction on the humidity bias could lead to improved aerosol optical properties at least for November and March during GVAX.

The effect of humidity bias in the boundary layer plays a greater role in AOD changes than the upper levels. Because aerosols are mainly concentrated near the surface layer, the same percentage change in RH would lead to a larger response in aerosols. In addition, as shown in Figure 4, the humidity effect on aerosol extinction is more significant at the surface than in the upper troposphere, which further enhances the influence of humidity

Table 1. Monthly mean aerosol optical depth (AOD) at Nainital from the default WRF-Chem model (control run), model output corrected by the RH bias (adjusted), GVAX MFRSR retrievals, and AERONET data from August 2011 to March 2012

	August	September	October	November	December	January	February	March
AOD (control run)	0.2688	0.134	0.186	0.0684	0.0648	0.1158	0.1451	0.1782
AOD (adjusted)	0.2947	0.1524	0.2551	0.1056	0.1192	0.1169	0.1327	0.2569
AOD (MFRSR)	–	0.1386	0.1843	0.0968	0.0752	0.1064	0.1676	0.2323
AOD (AERONET)	–	–	–	0.0979	0.0633	0.1137	0.1522	0.2383

bias in the lower troposphere on AOD. Since the model simulations of RH profiles have consistently dry biases near the surface during GVAX, the reduced humidity biases lead to increases in AOD at Nainital.

Summary and conclusion

The present study compares the relative humidity profiles and column precipitable water from regional WRF-Chem model and/or global NCEP reanalysis data with the GVAX observational data at Nainital, northern India and at TVM, southern India. The seasonal changes in the moist fields by altitude from the post-monsoon to the winter and spring months are captured by the large-scale model results. A wet bias in the middle and upper troposphere is generally simulated by the regional model, but a large dry bias is shown in the boundary-layer results. We further show that these moist biases, while significant, have a small impact on the WRF-Chem simulations of total water vapour due to the compensation effect in the lower atmosphere. The sign of the model biases over this region is consistent with other global climate model analysis of humidity biases[36]. While the higher-resolution regional model (WRF-Chem) performs better than the NCEP reanalysis at Nainital, it generates larger wet biases at TVM. The reasons for these location-dependent humidity biases in the models are unclear and deserve further investigation.

We have also examined the hypothesis that humidity bias contributes to the underestimation of simulated aerosol optical properties over the South Asia region. We find that, although the large wet bias in the upper troposphere might dominate the column water vapour overestimation, the boundary-layer humidity bias plays a more important role in AOD predictions. This effect is because aerosol loadings near the surface are higher, and more hygroscopic, and have a larger optical response to the relative humidity changes. Since most of the time a large dry bias is simulated in the boundary layer, this humidity bias would result in the underestimation of AOD, among other factors discussed.

1. Ramanathan, V. *et al.*, Indian Ocean Experiment: an integrated analysis of the climate forcing and effects of the great Indo-Asian haze. *J. Geophys. Res.*, 2001, **106**(D22), 28371–28398.
2. Di Girolamo, L. *et al.*, Analysis of Multi-Angle Imaging Spectro Radiometer (MISR) aerosol optical depths over greater India during winter 2001–2004. *Geophys. Res. Lett.*, 2004, **31**, L23115; doi:10.1029/2004GL021273.
3. Satheesh, S. K., Moorthy, K. K., Babu, S. S., Vinoj, V. and Dutt, C. B. S., Climate implications of large warming by elevated aerosol over India. *Geophys. Res. Lett.*, 2008, **35**, L19809; doi: 10.1029/2008GL034944.
4. Moorthy, K. K., Babu, S. S., Manoj, M. R. and Satheesh, S. K., Buildup of aerosols over the Indian region. *Geophys. Res. Lett.*, 2013, **40**, 1011–1014.
5. Ramana, M. V., Ramanathan, V., Kim, D., Roberts, G. C. and Corrigan, C. E., Atmospheric solar absorption and heating rate measurements with stacked UAVs. *Q. J. R. Meteor. Soc.*, 2007, **133**, 1913–1931.
6. Satheesh, S. K. *et al.*, Vertical structure and horizontal gradients of aerosol extinction coefficients over coastal India inferred from airborne lidar measurements during the integrated campaign for aerosol, gases and radiation budget (ICARB) field campaign. *J. Geophys. Res.*, 2009, **114**, D05204; doi:10.1029/2008JD011033.
7. Gautam, R., Hsu, N. C. and Lau, K.-M., Pre-monsoon aerosol characterization and radiative effects over the Indo-Gangetic Plains: implications for regional climate warming. *J. Geophys. Res.*, 2010, **115**, D17208; doi:10.1029/2010JD013819.
8. Carmichael, G. R. *et al.*, Asian aerosols: current and year 2030 distributions and implications to human health and regional climate change. *Environ. Sci. Technol.*, 2009, **43**, 5811–5817.
9. Ramanathan, V. and Carmichael, G., Global and regional climate changes due to black carbon. *Nature Geosci.*, 2008, **1**, 221–227.
10. Ramanathan, V., Ramana, M. V., Roberts, G., Kim, D., Corrigan, C., Chung, C. and Winker, D., Warming trends in Asia amplified by brown cloud solar absorption. *Nature*, 2007, **448**, 575–578.
11. Xu, B. Q. *et al.*, Black soot and the survival of Tibetan glaciers. *Proc. Natl. Acad. Sci. USA*, 2009, **106**(52), 22114–22118.
12. Ramanathan, V. *et al.*, Atmospheric brown clouds: regional assessment report with focus on Asia, United Nations Environment Programme, Nairobi, Kenya, 2008; http://www.rrcap.unep.org/abc/impact/
13. Chung, C. E. *et al.*, Anthropogenic aerosol radiative forcing in Asia derived from regional models with atmospheric and aerosol data assimilation. *Atmos. Chem. Phys.*, 2010, **10**, 6007–6024.
14. Boucher, O. *et al.*, Clouds and aerosols. In Climate Change 2013: The Physical Science Basis: Contribution of Working Group I to the Fifth Assessment Report of the Intergovernmental Panel on Climate Change (eds Stocker, T. F. *et al.*), Cambridge University Press, Cambridge, United Kingdom, 2013.
15. Pan, X. *et al.*, A multi-model evaluation of aerosols over South Asia: common problems and possible causes. *Atmos. Chem. Phys. Discuss.*, 2014, **14**, 19095–19147.
16. Nair, V. S., Solmon, F., Giorgi, F., Mariotti, L., Babu, S. S. and Moorthy, K. K., Simulation of South Asian aerosols for regional climate studies. *J. Geophys. Res.*, 2012, **117**, D04209; doi: 10.1029/2011JD016711.
17. Kumar, R., Barth, M. C., Pfister, G. G., Naja, M. and Brasseur, G. P., WRF-Chem simulations of a typical pre-monsoon dust storm in northern India: influences on aerosol optical properties and radiation budget. *Atmos. Chem. Phys.*, 2014, **14**, 2431–2446.

18. Koch, D. *et al.*, Evaluation of black carbon estimations in global aerosol models. *Atmos. Chem. Phys.*, 2009, **9**, 9001–9026.
19. Ganguly, D., Rasch, P. J., Wang, H. and Yoon, J., Climate response of the South Asian monsoon system to anthropogenic aerosols. *J. Geophys. Res*., 2012, **117**, D13209; doi:10.1029/2012JD017508.
20. Feng, Y., Kotamarthi, V. R., Coulter, R., Zhao, C. and Cadeddu, M., Radiative and thermodynamic responses to aerosol extinction profiles during the pre-monsoon month over South Asia. *Atmos. Chem. Phys.*, 2016, **16**, 247–264.
21. Lu, Z., Zhang, Q. and Streets, D. G., Sulfur dioxide and primary carbonaceous aerosol emissions in China and India 1996–2010. *Atmos. Chem. Phys*., 2011, **11**, 9839–9839.
22. Yevich, R. and Logan, J. A., An assessment of biofuel use and burning of agricultural waste in the developing world. *Global Biogeochem. Cycles*, 2003, **17**(4), 1095.
23. Ginoux, P., Chin, M., Tegen, I., Prospero, J. M., Holben, B., Dubovik, O. and Lin, S. J., Sources and distributions of dust aerosols simulated with the GOCART model. *J. Geophys. Res. Atmos*., 2001, **106**, 20255–20273.
24. Chin, M. *et al.*, Tropospheric aerosol optical thickness from the GOCART model and comparisons with satellite and sunphotometer measurements. *J. Atmos. Sci.*, 2002, **59**, 461–483.
25. Fast, J. D., Gustafson Jr, W. I., Easter, R. C., Zaveri, R. A., Barnard, J. C., Chapman, E. G. and Grell, G. A., Evolution of ozone, particulates, and aerosol direct forcing in an urban area using anew fully-coupled meteorology, chemistry, and aerosol model. *J. Geophys. Res.*, 2006, **111**, D21305; doi:10.1029/2005JD006721.
26. Petters, M. D. and Kreidenweis, S. M., A single parameter representation of hygroscopic growth and cloud condensation nucleus activity. *Atmos. Chem. Phys.*, 2007, **7**, 1961–1971.
27. Iacono, M. J., Delamere, J. S., Mlawer, E. J., Shephard, M. W., Clough, S. A. and Collins, W. D., Radiative forcing by long-lived greenhouse gases: calculations with the AER radiative transfer models. *J. Geophys. Res.*, 2008, **113**, D13103.
28. Zhao, C., Liu, X., Ruby, L. L. and Hagos, S., Radiative impact of mineral dust on monsoon precipitation variability over West Africa. *Atmos. Chem. Phys*., 2011, **11**, 1879–1893.
29. Thompson, G., Field, P. R., Rasmussen, R. M. and Hall, W. D., Explicit forecasts of winter precipitation using an improved bulk microphysics scheme. Part II: Implementation of a new snow parameterization. *Mon. Weather Rev.*, 2008, **136**, 5095–5115.
30. Zhang, G. J. and McFarlane, N. A., Sensitivity of climate simulations to the parameterization of cumulus convection in the Canadian Climate Centre general circulation model. *Atmos. Ocean*, 1995, **33**, 407–446.
31. Emmons, L. K. *et al.*, Description and evaluation of the model for ozone and related chemical tracers, version 4 (MOZART-4). *Geosci. Model Dev*., 2010, **3**, 43–67.
32. Raju, C. S., Renju, R., Antony, T., Mathew, N. and Moorthy, K. K., Microwave radiometric observation of a waterspout over coastal Arabian sea. *IEEE Geosci. Remote Sensing Lett.*, 2013, **10**(5), 1075–1079.
33. Renju, R., Raju, C. S., Mathew, N., Antony, T. and Krishna Moorthy, K., Microwave radiometer observations of interannual water vapor variability and vertical structure over a tropical station. *J. Geophys. Res. Atmos.*, 2015, **120**, 4585–4599.
34. Penner, J. E. *et al.*, A comparison of model- and satellite-derived aerosol optical depth and reflectivity. *J. Atmos. Sci.,* 2002, **59**, 441–460.
35. Govardhan, G., Nanjundiah, R. S., Satheesh, S. K., Krishnamoorthy, K. and Kotamarthi, V. R., Performance of WRF-Chem over Indian region: Comparison with measurements. *J. Earth Syst. Sci.*, 2015, **124**, 875–896.
36. John, V. O. and Soden, B. J., Temperature and humidity biases in global climate models and their impact on climate feedbacks. *Geophys. Res. Lett.*, 2007, **34**, L18704; doi: 10.1029/2007GL030429.

ACKNOWLEDGEMENTS. This work was supported by the US Department of Energy (DOE) as part of the Atmospheric System Research Program. Support for this research was provided to Y.F., V.R.K. and M.C. by Argonne National Laboratory under US DOE contract DE-AC02-06CH11357. All the numerical simulations were performed using the computing cluster (Fusion) operated by Argonne's Laboratory Computing Resource Center. R.R. and C.S.R. acknowledge Dr K. Krishnamoorthy and Dr S. K. Satheesh for GVAX data as well as scientific discussions.

doi: 10.18520/cs/v111/i1/93-100